PERGAMON

Solid State Communications 121 (2002) 471–474

solid state communications

www.elsevier.com/locate/ssc

Phonon dispersion of carbon nanotubes

J. Maultzsch[a,*], S. Reich[a], C. Thomsen[a], E. Dobardžić[b], I. Milošević[b], M. Damnjanović[b]

[a]*Institut für Festkörperphysik, Technische Universität Berlin, Hardenbergstr. 36, 10623 Berlin, Germany*
[b]*Faculty of Physics, University of Beograd, P.O. Box 368, Beograd 11001, Yugoslavia*

Received 21 December 2001; accepted 6 January 2002 by M. Cardona

Abstract

We present the phonon dispersion relations of single-wall carbon nanotubes calculated within a force-constants approach. By using the full symmetry group of the tubes, we are able to calculate the dispersion relations for any chirality starting from one single carbon atom. We find an overbending in the highest optical branch between 6 and 12 cm^{-1} independent of the tube diameter. The order of the high-energy modes at the Γ-point differs from the results derived from simple zone folding. The splitting between the two Raman active optical modes with A_1 symmetry at the Γ-point of chiral tubes is $\approx 4\ cm^{-1}$ for typical diameters; it increases with decreasing tube diameter.

PACS: 78.30; 63.22; 78.30.Na

Keywords: A. Carbon nanotubes; D. Phonons

The Raman spectra of single-wall carbon nanotubes are still being controversially discussed, despite the numerous studies in this field. Even recent experiments on isolated single tubes have not led so far to a full understanding of the observed Raman modes [1,2]. The interpretation of experimental data still relies on certain assumptions on the phonon frequencies derived from calculations. There are two main approaches in calculating the phonon dispersion of nanotubes. The first one is the so-called zone folding approximation, i.e. the graphene dispersion along the Brillouin zone lines corresponding to the states of the particular nanotube. Although this rather simple method can be used in principle for any nanotube, it suffers from several deficiencies. Curvature effects like different bond lengths and angles and rehybridization of the electronic π bonds are not taken into account, which may lead to incorrect predictions, especially for small tube diameters. In addition, the symmetry of the states is not completely obtained by zone folding, which affects selection rules essential for determining matrix elements. By definition, zone folding does not yield the nanotube-characteristic radial breathing mode, which, although derived from a graphene acoustic mode, has non-zero frequency at the Γ-point in nanotubes. Saito et al. have used a modified zone folding approach, taking the graphite force-constants but changing them such that the radial breathing mode was obtained [3]. In the second approach, the phonon dispersion is found by ab initio calculations. While this method is in general more reliable than zone folding with respect to curvature effects, it is (at this time) limited to achiral and to only a few chiral tubes with diameters $\lesssim 1$ nm because of the large number of atoms in the nanotube-unit cell. Sánchez-Portal et al. have shown that concerning the vibrational properties, the largest differences between ab initio calculations and zone folding occur in the low-energy range and for tubes with small diameters ($\lesssim 0.7$ nm) also in the high-energy range. The phonon frequencies soften with respect to the frequencies derived from graphene due to curvature effects [4]. So far, the calculations of phonon frequencies presented in the literature have focused mainly on armchair tubes or, if chiral tubes are considered, only on the Γ-point frequencies [3–5].

The Raman spectra of carbon nanotubes, however, appear to be dominated by defect-induced, double-resonant Raman scattering, which involves phonon wave vectors of the entire Brillouin zone. This was shown for the D mode [6] and, recently, for the entire (high-energy) Raman spectrum [7]. Therefore, complete, symmetry-based calculations of the full phonon dispersion for an arbitrary tube are necessary

* Corresponding author.
E-mail address: janina@physik.tu-berlin.de (J. Maultzsch).

0038-1098/02/$ - see front matter
PII: S0038-1098(02)00025-X

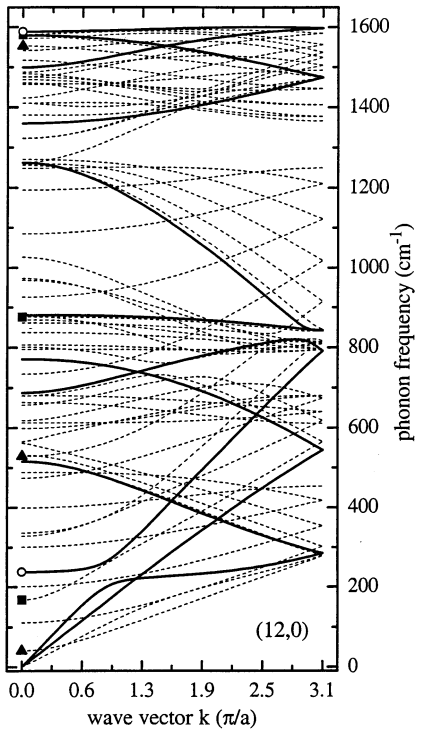

Fig. 1. Phonon dispersion of the (12,0) zig–zag tube. The bands with $m = 0$ and $m = n$ are given by bold lines. The symbols indicate the Raman active modes at the Γ-point; open circles denote A_{1g}, squares E_{1g} and triangles E_{2g} symmetry. The dashed lines are the bands with $m \in [1, n-1]$; they are four-fold degenerate for $k \in (0, \pi/a)$, where a is the length of the unit cell.

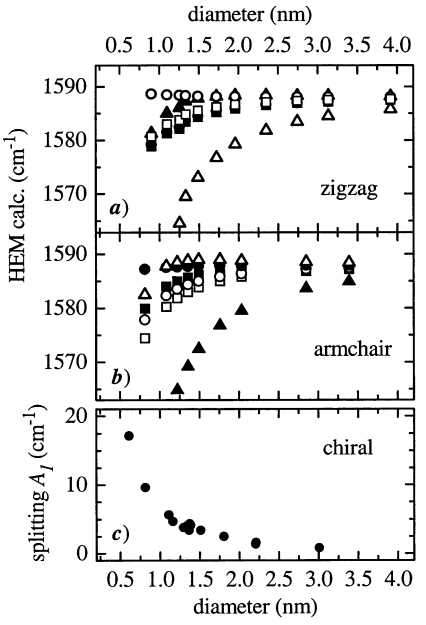

Fig. 2. (a) Γ-point frequencies of the high-energy bands of zig–zag tubes with $m = 0$ (circles), $m = 1$ (squares) and $m = 2$ (triangles) as a function of tube diameter. Open symbols indicate the Raman active modes. (b) Same as in (a), but for armchair tubes. (c) Splitting of the two high-energy Γ-point frequencies with A_1 symmetry in chiral tubes as a function of tube diameter.

for gaining further understanding of the Raman spectra and the vibrational properties in general.

Here, we present the phonon dispersion relations of both chiral and achiral isolated single-wall carbon nanotubes within a symmetry-based force-constants approach. We investigate the characteristics of the phonon dispersions relevant for the interpretation of Raman spectra and present their dependence on tube diameter and chirality.

A carbon nanotube is defined by the components (n_1, n_2) of the chiral vector, given in the basis of the graphene lattice vectors. The number of carbon atoms in the unit cell of the tube is $2q$, where $q = 2(n_1^2 + n_2^2 + n_1 n_2)/n\mathscr{R}$. n is the greatest common divisor of (n_1, n_2); $\mathscr{R} = 3$, if $(n_1 - n_2)/3n$ is integer, otherwise $\mathscr{R} = 1$ [8]. A carbon nanotube is a single-orbit system, i.e. the whole tube can be constructed from a single carbon atom by the application of all the symmetry operations of the nanotube group [9]. Therefore, the solution of any eigenvalue-problem can in principle be reduced to the solution in the low-dimensional interior space of one atom. By this approach we are able to calculate the phonon dispersion of any carbon nanotube, with no limitations caused by the large number of atoms in the unit cell as for chiral tubes. In addition, the phonons are automatically assigned by their full set of symmetry quantum numbers, including the parity with respect to the twofold rotational axis perpendicular to the tube axis and, for achiral tubes, the vertical and horizontal mirror planes. For the type of quantum numbers we choose both, the km numbers, describing separately the purely linear and angular momenta, and the helical $\tilde{k}\tilde{m}$ numbers, which are more convenient for the characterization of chiral tubes [9]. Calculations were performed using modified force-constants of graphite [10]. The change of the atom positions in the curved graphite sheet with respect to the flat graphene plane was incorporated by explicitly including the change in bond angle on the curved graphene wall. Additionally, we require vanishing energy of pure rotation around the tube axis (fourth acoustic mode). We included up to fourth nearest neighbor interaction in order to reproduce the experimentally observed overbending in the optical phonon bands. We verified the validity of our calculation by plotting the frequency of the radial breathing mode at the Γ-point (ω_{RBM}) as a function of inverse tube radius $1/r$ and found $(\omega_{\mathrm{RBM}}) = 1140\ \mathrm{cm}^{-1}$ Å averaged over all chiralities, which is well in the range found by other groups [4,10,11]. Note, that in our calculations the force-constants of graphite are not additionally manipulated in order to obtain the radial breathing mode as in other force-constants calculations [3].

In Fig. 1 we show the phonon dispersion of the (12,0) zig–zag tube. The bold lines are the doubly degenerate

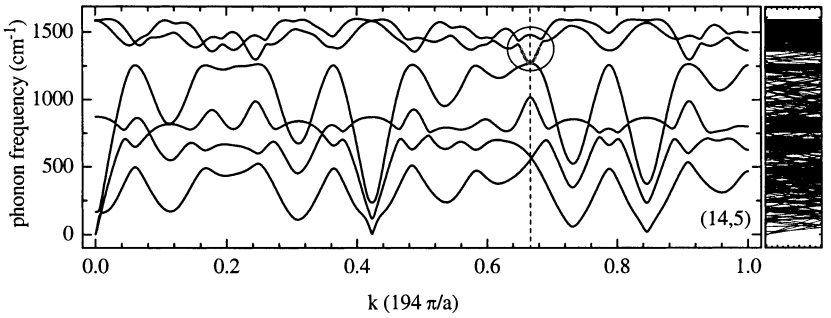

Fig. 3. Phonon dispersion of the (14,5) tube given by $\tilde{k}\tilde{m}$ quantum numbers. $q/n = 194$ and $\mathscr{R} = 3$. Because $n = 1$, $\tilde{m} = 0$, i.e. there are only six phonon bands. At 2/3 of the Brillouin zone (dashed line) there is a minimum in the optical branch at about 1250 cm^{-1} (grey line), which gives rise to the observed disorder Raman peak. Right: phonon dispersion of the (14,5) tube in linear quantum numbers; $m = -96, \ldots, 97$; the number of bands is 1164.

bands with angular momenta $m = 0$ and $m = n$, which contain the Γ- and M-point of graphene in the zone folding scheme. The symbols denote the Raman active modes at the Γ-point, where open circles indicate $A_{1g}({}_0A_0^+)$, squares $E_{1g}({}_0E_1^-)$ and triangles $E_{2g}({}_0E_2^+)$ symmetry. All other bands (dashed lines) are four-fold degenerate for $k \in (0, \pi/a)$ [8]. For the highest $m = 0$ optical branch the calculated overbending, i.e. the difference between the maximum and the Γ-point frequency, is about 12 cm^{-1}, which is in good agreement with experiments performed on bundled single-wall nanotubes [12]. The overbending does not depend on the diameter of the tube but decreases with increasing chiral angle towards 6 cm^{-1} for armchair tubes.

In the high-energy range, the order of the phonon frequencies at Γ is different from what is expected in the simple zone folding approach. The phonon frequency with $m = 0$ is the highest frequency; the $m = 2$ frequency appears slightly below (7 cm^{-1}). For zig–zag tubes with diameters larger than 1.49 nm [(19,0)], the upper two Γ-point frequencies interchange, see Fig. 2(a). We find the same behavior in armchair (Fig. 2(b)) and chiral tubes with the interchange of the $m = 0$ and $m = 2$ frequencies at a tube diameter of 1.09 nm for armchair tubes [(8,8)]. The frequency ordering of the high-energy bands is in good agreement with the calculations by Saito et al. [3]. The frequencies in the zone folding approach which originate from the transversal optical branch of graphene are sorted as expected, i.e. with decreasing frequency $m = 0$, 1, 2 for all tubes. While in chiral tubes there are six Raman active high-energy modes ($2A_1$, $2E_1$, $2E_2$), in achiral tubes only three of the high-energy modes are Raman active. These are, independent of the diameter, sorted by decreasing the frequency as E_{2g}, A_{1g}, E_{1g} and A_{1g}, E_{1g}, E_{2g} for armchair and zig–zag tubes, respectively, see Fig. 2. Therefore, besides selection rules, the high-energy peaks that are above the graphite Γ-point frequency cannot simply be assigned to E_{1g} and E_{2g} phonon modes as has been done, e.g. by Kasuya et al. [13].

From polarization-dependent Raman experiments on both

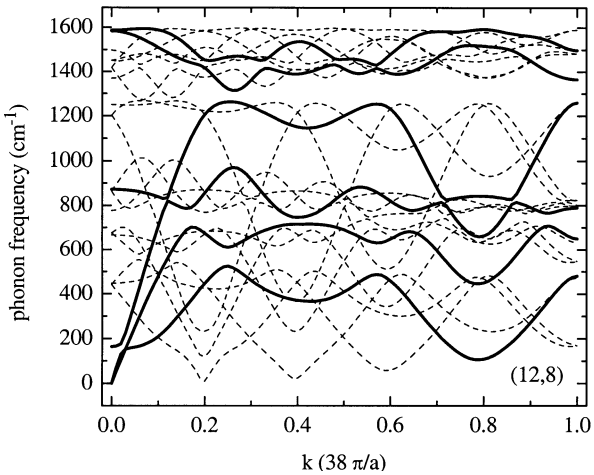

Fig. 4. Phonon dispersion of the (12,8) tube given by $\tilde{k}\tilde{m}$ quantum numbers. $\tilde{m}$ takes integer values from $-n/2 + 1$ to $n/2$, i.e. $\tilde{m} = -1, 0, 1, 2$. $q/n = 38$ and $\mathscr{R} = 1$. Bold lines indicate the bands with $\tilde{m} = 0$.

unoriented and aligned single-wall tubes, it is known that the phonon modes which contribute most to the Raman signal have A_{1g} (A_1) symmetry [1,14,15]. In Fig. 2(c) we plot the splitting of the two high-energy A_1 modes at the Γ-point of chiral tubes as a function of the tube diameter. The upper frequency slightly increases with decreasing diameter, whereas the lower frequency decreases with decreasing diameter. In our calculation, this splitting stems from the modified bond angles in the nanotube compared with the flat graphene sheet. In the diameter range between 1.1 and 1.5 nm, which covers the typical diameter range for experiments on single-wall nanotubes, the splitting of the A_1 modes is rather small, varying from ≈ 5 to $\approx 2\,\mathrm{cm}^{-1}$. In contrast, the peculiar high-energy peak structure in so-called semiconducting spectra exhibits a splitting of the peaks of $\approx 20\,\mathrm{cm}^{-1}$ with a peak width (FWHM) of ≈ 10–$20\,\mathrm{cm}^{-1}$, see for isolated tubes, e.g. Ref. [16]. Therefore, the high-energy spectra of carbon nanotubes cannot be explained simply by the splitting of the graphene degenerate optical modes into the non-degenerate nanotube modes at the Γ-point. In chiral tubes, the phonon modes in general do not have purely longitudinal or transversal character [17]. We thus do not expect other effects like rehybridization and dependence of the force-constants on the interatomic distance to further increase the splitting between the A_1 modes.

Representative for chiral tubes we show in Fig. 3 and in Fig. 4 the phonon dispersion of the (14,5) and the (12,8) tube, respectively, given by the helical $\tilde{k}\tilde{m}$ full quantum numbers. The length of the Brillouin zone is $(q\pi/na)$, which is $194\pi/a$ and $38\pi/a$ for the (14,5) and (12,8) tube, respectively. The bands with $\tilde{m}=0$ are given by the bold lines. A band with a given $\tilde{m}$ can be understood as 'unfolding' the bands in the km description by obeying the Umklapp rules at the zone boundary [18]. In contrast to m, $\tilde{m}$ is a fully conserved quantum number. As the phonon wave vectors participating in double-resonant Raman scattering can be large compared with the length of the 'helical' Brillouin zone $(q\pi/na)$, the use of $\tilde{k}\tilde{m}$ quantum numbers is more convenient than the use of the linear km quantum numbers and application of the Umklapp rules each time when crossing the zone boundary π/a. Besides, the number of bands is reduced by a factor of q/n in the $\tilde{k}\tilde{m}$ description, see Fig. 3. For the observation of the D mode, it is essential that there be a minimum in the $\tilde{m}=0$ branch around 2/3 of the Brillouin zone at the corresponding frequency [6]. Indeed, we find for the $\mathscr{R}=3$ (14,5) tube a minimum with a high density of states in one of the high-energy bands at 2/3 of the Brillouin zone with a frequency around $1250\,\mathrm{cm}^{-1}$. In contrast to graphene, the quasi acoustic and optical bands touching at 2/3 of the Brillouin zone do not cross in the tubes. Instead, they have a local maximum and minimum with a high phonon density of states. In particular, this might alter the intensity dependence of the D mode with varying laser energies, which should be taken into account in future studies of this disorder induced peak. In the $\mathscr{R}=1$ (12,8) tube, there is no minimum in the optical branches at 2/3 of the Brillouin zone. Considering the $\tilde{m}=0$ bands, there is even a gap around the expected D mode frequency. It can be easily proven that, in general, only tubes with $\mathscr{R}=3$ show this minimum at 2/3 of the Brillouin zone in one of the optical $\tilde{m}=0$ branches, see also Ref. [19].

In conclusion, we have presented the phonon dispersion relations of achiral and chiral tubes calculated within a symmetry-based force-constants approach. We showed that the splitting between the two Raman active high-energy modes with A_1 symmetry is too small to account for the splitting of the high-energy peaks observed in first-order Raman spectra. For chiral tubes, we confirmed the predicted differences between $\mathscr{R}=3$ and $\mathscr{R}=1$ tubes.

References

[1] G.S. Duesberg, I. Loa, M. Burghard, K. Syassen, S. Roth, Phys. Rev. Lett. 85 (2000) 5436.
[2] A. Jorio, R. Saito, J.H. Hafner, C.M. Lieber, M. Hunter, T. McClure, G. Dresselhaus, M.S. Dresselhaus, Phys. Rev. Lett. 86 (2001) 1118.
[3] R. Saito, T. Takeya, T. Kimura, G. Dresselhaus, M.S. Dresselhaus, Phys. Rev. B 57 (1998) 4145.
[4] D. Sánchez-Portal, E. Artacho, J.M. Soler, A. Rubio, P. Ordejón, Phys. Rev. B 59 (1999) 12678.
[5] A. Charlier, E. McRae, M.-F. Charlier, A. Spire, S. Forster, Phys. Rev. B 57 (1998) 6689.
[6] J. Maultzsch, S. Reich, C. Thomsen, Phys. Rev. B 64 (2001) 121407(R).
[7] J. Maultzsch, S. Reich, C. Thomsen, Phys. Rev. Lett. submitted.
[8] M. Damnjanović, I. Milošević, T. Vuković, R. Sredanović, Phys. Rev. B 60 (1999) 2728.
[9] M. Damnjanović, T. Vuković, I. Milošević, J. Phys. A 33 (2000) 6561.
[10] R.A. Jishi, L. Venkataraman, M.S. Dresselhaus, G. Dresselhaus, Chem. Phys. Lett. 209 (1993) 77.
[11] J. Kürti, G. Kresse, H. Kuzmany, Phys. Rev. B 58 (1998) R8869.
[12] C. Thomsen, Phys. Rev. B 61 (2000) 4542.
[13] A. Kasuya, Y. Sasaki, Y. Saito, K. Tohji, Y. Nishina, Phys. Rev. Lett. 78 (1997) 4434.
[14] A. Jorio, G. Dresselhaus, M.S. Dresselhaus, M. Souza, M.S.S. Dantas, M.A. Pimenta, A.M. Rao, R. Saito, C. Liu, H.M. Cheng, Phys. Rev. Lett. 85 (2000) 2617.
[15] S. Reich, C. Thomsen, G.S. Duesberg, S. Roth, Phys. Rev. B 63 (2001) R041401.
[16] M.A. Pimenta, A. Jorio, S.D.M. Brown, A.G.S. Filho, G. Dresselhaus, J.H. Hafner, C.M. Lieber, R. Saito, M.S. Dresselhaus, Phys. Rev. B 64 (2001) 041401(R).
[17] S. Reich, C. Thomsen, P. Ordejón, Phys. Rev. B 64 (2001) 195416.
[18] M. Damnjanović, I. Božović, N. Božović, J. Phys. A: Math. Gen. 17 (1984) 747.
[19] M. Damnjanović, T. Vuković, I. Milošević, Solid State Commun. 116 (2000) 265.